Ground-state properties of the three-dimensional Ising spin glass

Bernd A. Berg
Department of Physics, The Florida State University, Tallahassee, Florida 32306
and Supercomputer Computations Research Institute, Tallahassee, Florida 32306

Ulrich E. Hansmann
Supercomputer Computations Research Institute, Tallahassee, Florida 32306

Tarik Celik
Department of Physics, Hacettepe University, Ankara, Turkey
(Received 1 March 1994)

We study zero-temperature properties of the three-dimensional Edwards-Anderson Ising spin glass on finite lattices up to size 12^3. Using multicanonical sampling we generate large numbers of ground-state configurations in thermal equilibrium. Finite-size scaling fits of the data are carried out for two hypothetical scenarios: Parisi mean-field theory versus a droplet scaling ansatz. With a zero-temperature scaling exponent $y=0.72\pm0.12$ the data are well described by the droplet scaling ansatz. Alternatively, a description in terms of the Parisi mean-field behavior is still possible. The two scenarios give significantly different predictions on lattices of size $\geq 12^3$.

I. INTRODUCTION

The theoretical problem to determine the equilibrium ground-state structure of spin glasses has remained an important, but elusive, question. It is generally agreed that the statistical mechanics of the infinitely ranged Sherrington-Kirkpatrick (SK) Ising spin glass is essentially understood. The replica-symmetry-breaking mean-field (MF) scheme discovered by Parisi[1] exhibits infinitely many low-temperature states whose properties are consistent with simulations,[2] see Ref. 3 for a recent overview.

More realistic models rely on short-range interactions. The simplest prototype of this sort is the Edwards-Anderson Ising spin glass (EAI), defined by the Hamiltonian

$$H_J=-\sum_{\langle ij\rangle} J_{ij}s_i s_j \ . \tag{1}$$

Here the sum $\langle ij\rangle$ goes over nearest neighbors. We consider $3d$ systems with periodic boundary conditions and $N=L^3$ spins $s_i=\pm1$. The exchange interactions between the spins are taken $J_{ij}=\pm1$, randomly distributed over the lattice such that the constraint $\sum_{\langle ij\rangle}J_{ij}=0$ is fulfilled. The subscript J denotes the realization $\{J_{ij}\}$. Extensive numerical studies of this model were carried out in the past.[4-7] In essence, these simulations seem to have established the existence of a freezing phase transition, although not beyond all doubts.[8]

After the SK model had been solved it became a question of central theoretical interest whether, well below the freezing temperature $T_c=\beta_c^{-1}\approx1.2$,[6,7] the three-dimensional (3D) EAI spin-glass model exhibits Parisi MF behavior.[9] It was answered in the negative by proponents of a simple scaling ansatz.[10-15] These droplet scaling (DS) theories suggest that no more than two pure states (related via a global flip) exist at any temperature. The MF approximation is surely valid for $d\to\infty$. For the model at hand, with discrete exchange interactions, it has been suggested[15] that the MF scenario holds for $d\geq4$, whereas for $d=3$ there are just two pure states. For Gaussian distributed exchange interactions $d=6$ is conjectured[11,13] to be the upper critical dimension, which separates the MF from the DS scenario.

Simulations[16] in a magnetic field H seemed to favor the MF picture rather than the alternative droplet model. However, it has been pointed out that equilibrium at sufficiently low temperatures has not been reached,[17] and a recent Monte Carlo (MC) study[18] also disagrees with the conclusions of Ref. 16. A study of contours of the spin-glass susceptibility in the (H,T) plane as means of distinguishing the two pictures was performed in Ref. 19, but remained ambiguous in $d=3$. Finally, a recent investigation of the face-centered-cubic lattice[20] is consistent with the existence of an Almeida-Thouless line in the (H,T) plane and thus favors again the MF scenario.

In the present paper we employ multicanonical MC techniques[21-23] to shed new light on the spin-glass ground-state problem. In Sec. II, the observables used to characterize the spin-glass properties are introduced. The numerical results are then presented in Sec. III, and Sec. IV contains a few concluding remarks.

II. THE OBSERVABLES

For each system there are $(3N)!/[(3N/2)!]^2$ realizations of the quenched random variables $J=\{J_{ij}\}$. A quantity of decisive importance is the probability density $P(q)$ of the Parisi order parameter q:

$$P(q)=[P_J(q)]_{\rm av}=\frac{[(3N/2)!]^2}{(3N)!}\sum_J P_J(q) \ . \tag{2}$$

 ©1994 The American Physical Society

By $[\cdot]_{\rm av}$ we denote averaging over the realizations J, whereas $\langle\cdot\rangle_T$ denotes the thermal (time) average for a given realization of bonds. For such a fixed realization $P_J(q)$ is the probability density of the overlap

$$q=q_J=\frac{1}{N}\sum_i s_i^1 s_i^2\Big|_J \ . \tag{3}$$

Here s_i^1 and s_i^2 denote two replicas (i.e., statistically independent configurations) of the realization J at temperature T. Our normalization is

$$\int_{-1}^{+1}P(q)dq=\int_{-1}^{+1}P_J(q)dq=1 \ .$$

Due to the magnetic field being zero we have the symmetry $P(-q)=P(q)$, such that $\int_{-1}^{+1}q^nP(q)dq=0$ for n odd. We are therefore only interested in averages over the range $0\le q\le 1$:

$$\overline{|q|^n}=[\langle|q_J|^n\rangle_T]_{\rm av}=2\int_0^1 q^nP(q)dq \ . \tag{4}$$

Of course, $\overline{q^n}=[\langle q^n\rangle_T]_{\rm av}=\overline{|q|^n}$ for n even. For a fixed realization J the analogous averages are defined by

$$\overline{|q_J|^n}=\langle|q_J|^n\rangle_T=2\int_0^1 q^nP_J(q)dq \ . \tag{5}$$

In the infinite volume limit the overall scenario is that for MF theory $P(q)$ takes nonzero values in a continuous range $|q|<q_1$ with peaks at $\pm q_{\rm max}$ and $0<q_{\rm max}\le q_1$. We denote the value at the peak by $P_{\rm max}=P(q_{\rm max})=P(-q_{\rm max})$. If the DS picture is correct, only a double-peak structure survives in the infinite volume limit, i.e., $\lim_{L\to\infty}P(q)=0$ for $q\neq q_{\rm max}$, where $q_{\rm max}^{\infty}$ is the infinite volume limit of $q_{\rm max}^L$. Whenever, without confusion, possible, we drop the subscript denoting the lattice size.

Let us now discuss moments of the order-parameter distribution. For the spin-glass susceptibility $\chi_q=N\overline{q^2}$ the MF as well as the DS scenario suggest divergence $\chi_q\sim N$ for $T<T_c$. However, they give significantly different predictions for the variance

$$\sigma^2(|\bar q|)=2\int_0^1(|\bar q|-q)^2P(q)dq=\overline{q^2}-\overline{|q|^2} \ . \tag{6}$$

Let us temporarily confine the discussion to zero temperature. In the limit $L\to\infty$ one has $\sigma^2(\overline{|q|})\to$finite in MF theory, while $\sigma^2(\overline{|q|})\sim L^{-y}\to 0$ within the DS approach. Here $y=-y_T$ is the zero-temperature scaling exponent,[11,13] denoted θ in Refs. 12 and 14. Within the DS ansatz it is supposed to govern quite generally the finite-size-scaling (FSS) corrections of expectation values. For instance, for the moments $|q|_L^n-|q|_\infty^n\sim L^{-y}$, or for the position of the maximum $q_{\rm max}^L-q_{\rm max}^\infty\sim L^{-y}$. For MF theory we assume for most of our fits 1/Volume corrections. The assumption of exponentially small volume corrections may be even more appropriate. However, this introduces one more fit parameter and presently we have not sufficiently many lattice sizes to allow its determination self-consistently. By this reason exponentially small corrections are only explored once (for the energy).

Assuming DS, the above zero-temperature scaling exponent should also govern the falloff of the probability density $P(q)$ for q away from $q_{\rm max}^\infty$. For instance, $P_L(0)\sim L^{-y}$. However, numerically it is rather tedious to get sufficiently good statistics at a particular q value. It is more convenient to rely on the probability distribution

$$x(q)=2\int_0^q P(q')dq' \ , \tag{7}$$

where $q<q_{\rm max}$ should stay sufficiently far away from $q_{\rm max}$. It is clear that the FS behavior is still $x_L(q)\sim L^{-y}$, but the statistical noise will be considerably suppressed.

Lack of self-averaging is one prominent feature of MF behavior. This means physical quantities Q exist for which

$$\lim_{L\to\infty}[(\bar Q-\bar Q_J)^2]_{\rm av}\neq 0 \tag{8}$$

holds. In Ref. 16 the probability density itself was studied through $[\int[P(q)-P_J(q)]^2dq]_{\rm av}$. This was criticized by the authors of Ref. 17 on the reason that the probability density is so singular that it would be non-self-averaging in the DS picture too. Following their suggestion we estimate

$$\sigma_J^2(\overline{q^2})=[(\overline{q^2}-\overline{q_J^2})^2]_{\rm av}=[(\overline{q_J^2})^2]_{\rm av}-(\overline{q^2})^2 \ . \tag{9}$$

Again, this quantity stays finite in MF theory, but drops off $\sim L^{-y}$ in the DS picture.

In contrast to this, standard thermodynamical quantities like the energy per spin e or the entropy per spin s are self-averaging in both scenarios:

$$e=N^{-1}[\langle H_J\rangle_T]_{\rm av}=N^{-1}\langle H_J\rangle_T \tag{10}$$

and

$$\begin{aligned}s&=N^{-1}\frac{\partial}{\partial T}(T[\langle\ln Z_J\rangle_T]_{\rm av})\\&=N^{-1}\frac{\partial}{\partial T}(T\langle\ln Z_J\rangle_T) \ ,\end{aligned} \tag{11}$$

where Z_J is the partition function for realization J. The multicanonical method allows one, including proper normalization, to evaluate the partition function and its derivatives numerically.

III. NUMERICAL RESULTS

With the development of multicanonical techniques for disordered systems[23] it has become feasible to generate spin-glass ground states in thermal equilibrium; see Ref. 24 for a brief, general review, Ref. 25 for the earlier umbrella sampling, and Refs. 26–28 for the related simulated tempering. A pilot study for the model at hand has been presented in Ref. 29. In essence a multicanonical spin-glass simulation proceeds in three steps. First Monte Carlo weights are recursively constructed[30] which will allow one to simulate an ensemble, the "multicanonical," which yields canonical expectation values in the temperature range $0\le T\le\infty$ through use of the spectral density. Second, equilibrium configurations with respect to the multicanonical ensemble are generated by means of standard MC. In a third step canonical expectation values at desired temperatures are obtained from the analysis. Multicanonical sampling circumvents the no-

torious ergodicity problems of canonical low-temperature spin-glass simulations through regular excursions into the disordered phase, *while* staying in equilibrium.

In this paper we focus on the investigation of ground-state properties. A lower bound on the number of statistically independent ground states sampled is obtained by counting how often the system moves from the energy $E \geq 0$ region to the ground-state energy $E_{\min}$, and back to the $E \geq 0$ region. This has been termed "tunneling"[22] and we follow this notation, but one should bear in mind that the free-energy barriers are actually not overcome by a tunneling process. Our tunneling time τ is the average number of single-spin updates corresponding to one tunneling event.

We will interpret our data through FSS fits of our measured quantities. The DS scenario implies that the leading-order FS corrections are governed by the zero-temperature scaling exponent y. Less clear are the leading FS corrections to MF theory. The exactly solvable random energy model[31] was constructed to exhibit properties typical for long-range interactions of the SK type. It exhibits 1/Volume leading corrections at $T=0$. A two-parameter fit of this type is what we assume, with one exception, throughout this paper. For the energy itself, this turns out to be inconsistent with the data. A consistent fit is still possible, if one assumes exponentially small corrections in L ($V=N=L^3$), which require a three-parameter fit. This would be typical for noncritical short-range interactions. Each spin "sees" the periodic boundary only via exponentially decaying correlations. Unfortunately, our limitation to rather small sized lattices prohibits a self-consistent estimate of the leading correction from the data.

A. Statistics and slowing down

We have performed simulations for $L=4$, 6, 8, 12 ($N=64$, 216, 512, 1728). For $L \leq 8$ the sum (2) is approximated through 512 randomly chosen realizations of the $\{J_{ij}\}$, whereas we have only 7 realizations for $L=12$. For all 1543 cases multicanonical parameters were determined recursively. Then each system was simulated twice with independent random starts and random numbers. This constitutes our two independent replica per realization. In these production runs iterations were stopped when a preset number of tunneling events n_τ had occurred: $n_\tau=128$ ($L=4$), 64 ($L=6$), 32 ($L=8$), and 10 ($L=12$). Despite this decrease in tunneling events, the average number of updates per spin n_s (sweeps) did steadily increase. Approximate values are $n_s=8\times10^4$ ($L=4$), 10^5 ($L=6$), 7.6×10^6 ($L=8$), and 50×10^6 ($L=12$). The average CPU time spent on one $L=8$ replica was approximately 800 min on an IBM 320H workstation.

Per replica we have stored up to 2048 ground-state configurations. Due to correlations the number of encountered ground states is, of course, much larger than n_τ. If the number exceeded 2048, the stored configurations were randomly selected from the total set. For ground-state configuration n this is elegantly done on line by picking a random integer i_r in the range $1 \leq i_r \leq n$. Configuration n is stored at position i_r if $i_r \leq 2048$ and discarded otherwise. For both replica the same ground-state energy has to be found between all tunneling counts. This is a strong, albeit not rigorous, criterium to ensure that the correct ground-state energy has not been missed. Indeed, in course of a study,[32] aimed at improving the algorithmic performance, lower-energy states have been found for a few of the $L=8$ and 12 configurations used in this paper. In all $L=8$ cases the improvement is just by a single energy step, and the indication is that it happens for less than 2% of our recorded configurations. Comparing the ground-state properties of the old and new configurations shows that the presently implied bias favors the MF picture, but is negligible within the statistical noise due to the small number of configurations affected. For $L=12$ the problem is more serious, but they are anyhow of limited relevance to the subsequent discussion. No improvements were found for any $L=4$ or 6 configurations.

Table I presents our zero-temperature estimates for observables introduced in the previous section. The error bars are with respect to the different realizations, which are statistically independent and enter with equal

TABLE I. Data.

	$L=4$	$L=6$	$L=8$	$L=12$
τ	398*E*2(15E2)	336*E*4(30E4)	171*E*6(46E6)	139*E*8(77E8)
$-e$	1.737 8(28)	1.767 4(13)	1.779 9(08)	1.793 6(27)
s	0.074 0(09)	0.053 5(05)	0.047 9(03)	0.043 7(24)
$\sigma^2(e)$	0.003 73(25)	0.000 749(51)	0.000 277(19)	0.000 057(34)
$\sigma^2(s)$	0.000 784(53)	0.000 190(13)	0.000 070 9(48)	0.000 046(27)
$\lvert\bar{q}\rvert$	0.785(07)	0.800(06)	0.817(06)	0.880(28)
$\bar{q^2}$	0.669(09)	0.685(08)	0.703(07)	0.786(38)
$q_{\max}$	0.939(06)	0.925 2(25)	0.916 0(15)	0.901(10)
$P_{\max}$	4.08(15)	6.04(21)	8.38(26)	16.0(5.0)
$P(0)$	0.206 (30)	0.231 (41)	0.140 (37)	0.007 (07)
$x(\frac{1}{2})$	0.265(17)	0.204(15)	0.160(15)	0.042(42)
$\sigma^2(\bar{q})$	0.053 2(26)	0.044 6(27)	0.035 4(27)	0.013(13)
$\sigma_J^2(q^2)$	0.038 5(17)	0.025 8(15)	0.021 4(15)	0.006(06)

weights. Let us first discuss the slowing down as inferred from the FS behavior of the tunneling time τ. A formal, linear fit corresponding to the power law $\tau = a_1 V^{a_2}$ gives $a_2 = 3.8 \pm 0.1$ and is depicted in Fig. 1. This is a bit worse than our preliminary estimate[29] $a_2 = 3.4 \pm 0.2$. In addition, the fit is somewhat ambiguous because the distribution of the τ_L with respect to different realizations J is not Gaussian (for a fixed realization it is trivially Poison). This obscures, at least for $L = 8$ and 12, the meaning of the error bars entering this fit. A more detailed analysis[32] indicates that exponential slowing down, due to some particularly bad realizations, may still be feasible. Presently the $\sim V^{3.8}$ slowing down has limited our investigation to rather moderately sized lattices.

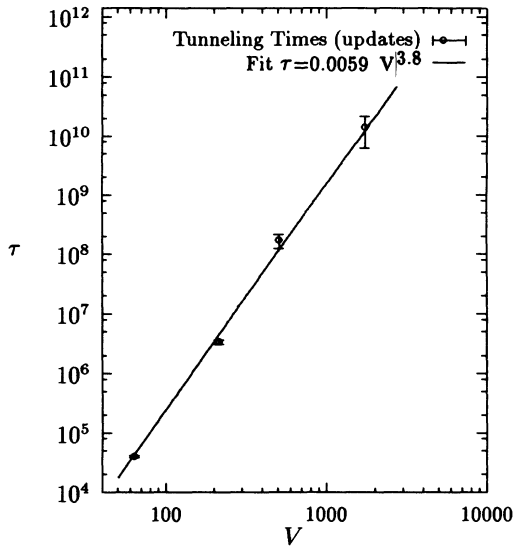

FIG. 1. Tunneling time vs lattice size L^3 on a double log scale.

B. Parisi order-parameter distribution

On a semilog scale Fig. 2 depicts the obtained zero-temperature probability densities (2) for the Parisi order parameter. The $L = 12$ probability density, presented without error bars, is very bumpy due to the small number of realizations, and may only be reliable for a few of the considered physical quantities. Note, altogether the data respect the $P(q) = P(-q)$ symmetry well. For $L = 8$, Fig. 3 plots the $P_J(q)$ probability densities of two rather extreme $L = 8$ realizations: two peak shape versus continuous distribution. Various different shapes in between these extremes are also found. Figure 4 shows all $L = 8$ realizations together. From Figs. 2–4 it is evident that only a careful quantitative analysis of these distributions may give hints concerning the $L \to \infty$ ground-state distribution.

Table II summarizes two-parameter fits of the data from Table I, assuming alternatively MF theory or the DS ansatz to be true. If MF and DS scenario lead to the same functional form, the fit is marked "All." The ∞ column gives the infinite volume extrapolations of the considered quantity, Q is the goodness of fit,[33] and R_{12} comments "Yes" or "No" on the reliability of the $L = 12$ data for the purposes of the particular fit. With an exception for $P_{\max}$, the MF and ALL fits are of the form $a_1 + a_2/L^3$, whereas the DS fits are either of the form $a_1 L^{-a_2}$ ($y = a_2$), or, when the zero-temperature scaling exponent is already determined, of the form $a_1 + a_2 L^{-y}$.

Let us first discuss $P_{\max}$. In the MF as well as in the DS scenario the self-overlap gives rise to a δ-function singularity. Therefore $P_{\max}$ is supposed to grow $\sim V$ and the appropriate fit is $a_1 L^3 + a_2$. Including all data points

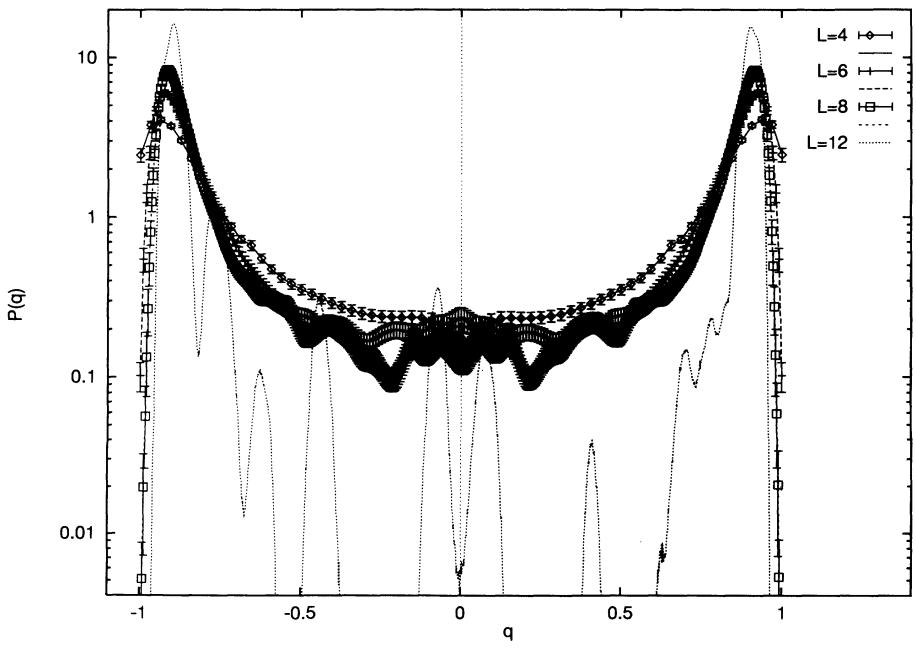

FIG. 2. Probability densities $P(q)$ for the Parisi order parameter ($L = 4$, 6, 8, and 12).

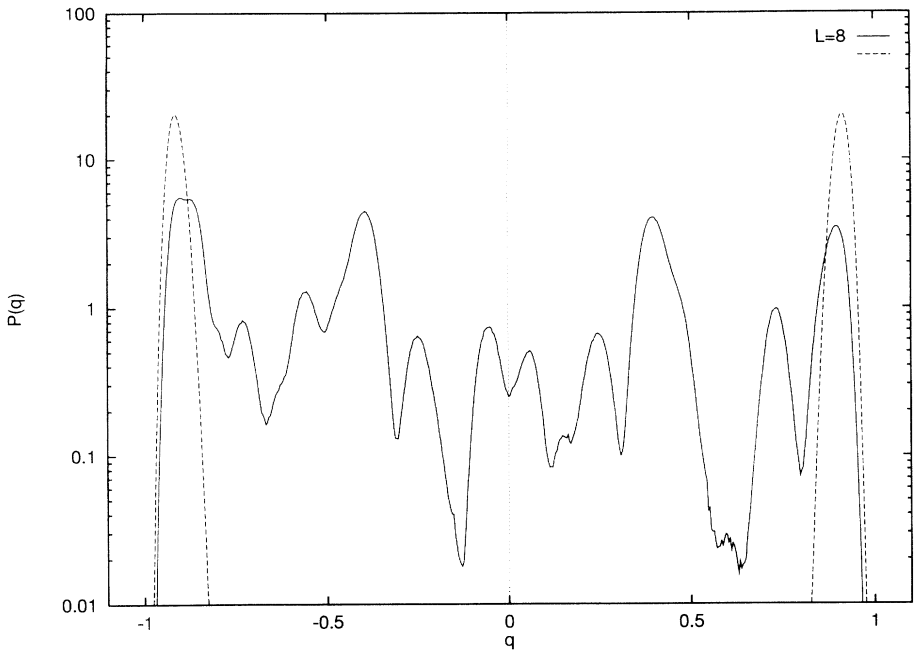

FIG. 3. Probability densities $P_J(q)$ for two very different $L=8$ realizations.

the fit is still consistent. Although, omitting the smallest lattice indicates that $L=4$ may not fully exhibit the asymptotic behavior.

Let us now discuss $\sigma^2(|\overline{q}|)$ and $\sigma_J^2(\overline{q^2})$. The DS fit is $a_1 L^{-a_2}$. Fits and data are depicted in Fig. 5. For each case we give two fit curves. The upper one relies on three data points ($L=4,6,8$), whereas the lower one includes also the $L=12$ result. When only three data are used, MF and DS fits are both consistent ($Q=0.10$ and 0.43). Once the $L=12$ data point is included, the consistency of the MF fit becomes marginal ($Q=0.04$). However, from the $L=8$ data we have the experience that 10% of the realizations amount to 99% of the $P(0)$ contribution. Consequently, the $L=12$ data suffer not only from large statistical fluctuations, but are altogether unreliable for quantities which are sensitive to the small-q distribution. We now rely on the three-point fits for $\sigma^2(|\overline{q}|)$ and $\sigma_J^2(\overline{q^2})$. The two $y=a_2$ estimates are still compatible, and we summarize them to

$$y=0.72\pm0.12\ . \tag{12}$$

The error bar is not reduced as both estimates rely on the

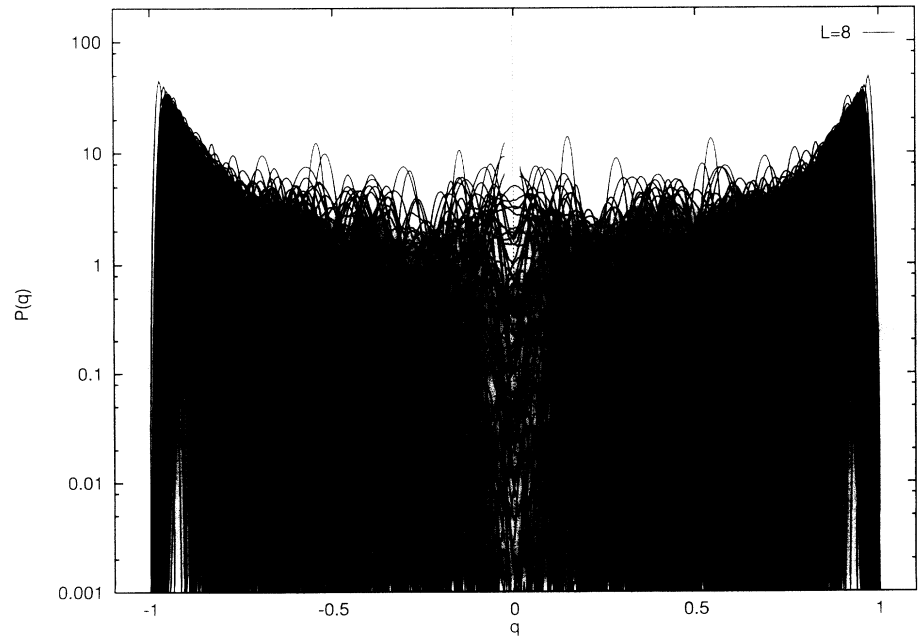

FIG. 4. All $P_J(q)$ probability densities for $L=8$.

TABLE II. Fits as defined in the text.

	∞	a_1 $L=4\rightarrow 8t$	a_2	Q	a_1 $L=4\rightarrow 12t$	a_2	Q	R_{12}	Fit
$-e$	a_1	1.785 41(92)	−3.23(21)	0.01	1.786 37(88)	−3.23(21)	10^{-5}	Y	MF
$-e$	a_1	1.840 51(42)	−0.279(18)	0.16	1.838 9(40)	0.274(16)	0.29	Y	DS
s	a_1	0.044 19(46)	1.947(97)	0.49	0.044 13(46)	1.954(97)	0.64	Y	All
$L^3\sigma^2(e)$	a_1	0.128(10)	7.1(1.4)	0.94	0.128(10)	7.2(1.4)	0.85	Y	All
$L^3\sigma^2(s)$	a_1	0.035 2(25)	0.98(31)	0.56	0.035 3(25)	0.97(31)	0.55	Y	All
$\overline{\lvert q\rvert}$	a_1	0.816 8(53)	−2.18(62)	0.20	0.819 6(51)	−2.41 62)	0.01	N	MF
$\overline{\lvert q\rvert}$	a_1	0.863(17)	−0.225 (61)	0.44	0.873(16)	−0.258(59)	0.09	N	DS
$\overline{q^2}$	a_1	0.702 9(64)	−2.32(78)	0.20	0.705 9(63)	−2.58(78)	0.02	N	MF
$\overline{q^2}$	a_1	0.752(21)	−0.239(76)	0.48	0.764(20)	−0.278(74)	0.08	N	DS
$q_{\max}$	a_1	0.913 5(20)	1.82(42)	0.12	0.912 9(19)	1.90(42)	0.09	Y	MF
$q_{\max}$	a_1	0.880 8(85)	0.165(36)	0.73	0.879 1(81)	0.171(34)	0.77	Y	DS
$P_{\max}$	∞	3.58(17)	0.009 74(67)	0.04	3.60(17)	0.009 58(65)	0.08	Y	All
$P_{\max}$	∞		$L=6,8,12$:	$\rightarrow$	4.39(39)	0.007 7(11)	0.66	Y	All
$P(0)$	a_1	0.168(35)	2.8(3.3)	0.13	0.002(07)	14.9(2.1)	10^{-6}	N	MF
$P(0)$	0	0.36 (22)	0.38(36)	0.17	0.76(39)	1.21(24)	10^{-11}	N	DS
$x(\frac{1}{2})$	a_1	0.157(15)	7.1(1.6)	0.23	0.146(13)	8.1(1.6)	0.12	N	MF
$x(\frac{1}{2})$	0	0.71(19)	0.71(16)	0.73	0.82(21)	0.80(15)	0.19	N	DS
$\sigma^2(\overline{\lvert q\rvert})$	a_1	0.035 9 (25)	1.15 (25)	0.10	0.034 9 (25)	1.22 (26)	0.04	N	MF
$\sigma^2(\overline{\lvert q\rvert})$	0	0.116(24)	0.55(13)	0.43	0.123(25)	0.59(12)	0.28	N	DS
$\sigma_J^2(\overline{q^2})$	a_1	0.019 5(15)	1.23(16)	0.59	0.018 8(14)	1.28(16)	0.06	N	MF
$\sigma_J^2(\overline{q^2})$	0	0.129(25)	0.88(12)	0.44	0.137(26)	0.92(12)	0.29	N	DS

same data set. It should be noted that the estimates of the literature correspond to a Gaussian distribution of the exchange coupling and that the discrete distribution constitutes a different universality class.[13]

The above fits were also used for $P(0)$, but the data are too inaccurate to yield meaningful results. As discussed, this is different for the distribution function $x(q)$ with an appropriate choice for q. Our smallest FSS extrapolation of $q_{\max}^{\infty}$ is 0.8791 ± 0.0081 (Table II). Therefore $q=\frac{1}{2}$ is certainly an appropriate choice. Table I includes our numerical estimates for $x(\frac{1}{2})$. It should be noted that for $L=12$ the error bar matches the estimated value, because the entire contribution to $x(\frac{1}{2})$ comes [as for $P(0)$] from a single realization. Table II contains the FSS fits for $x(\frac{1}{2})$ which we also display in Fig. 6. Relying on three lattices again, it is quite satisfying that the obtained zero-temperature exponent $y=0.71\pm0.16$ is in excellent

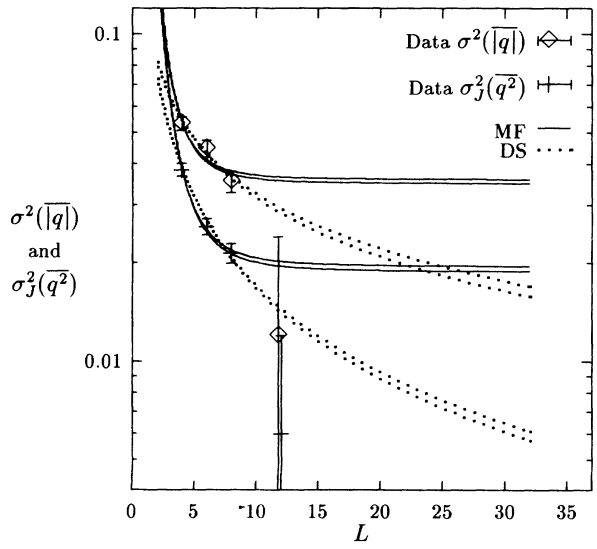

FIG. 5. Fits for $\sigma^2(\overline{\lvert q\rvert})$ and $\sigma_J^2(\overline{q^2})$. They rely either on the mean-field (MF) or on the droplet scaling (DS) scenario. For each case there are two fits, such that the lower one includes the (unreliable) $L=12$ data.

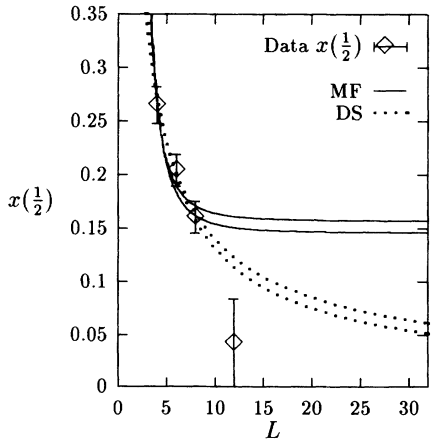

FIG. 6. Fits for $x(\frac{1}{2})$. They rely either on the mean-field (MF) or on the droplet scaling (DS) scenario. For each case there are two fits, such that the lower one includes the (unreliable) $L=12$ data point.

agreement with Eq. (12).

Assuming that our $L=4-8$ lattices show already typical scaling behavior, we conclude from Figs. 5 and 6 that similarly accurate data on lattices up to size $L=16$ would discriminate between the MF and the DS ansatz. Due to the $\sim V^{3.8}$ slowing down the needed CPU time would be about 3000 times larger than the one spent on the present investigation. With upcoming massively parallel devices in the teraflop range such a factor can be achieved.

The DS fits for $\bar{q}, \bar{q}^2$ and $q_{\max}$ in Table II are of the form $a_1+a_2L^{-y}$, where the exponent $y=0.72$ (12) is now used as input. The corresponding MF fits are of the form $a_1+a_2L^{-3}$. A relevant consistency check for the correctness of the DS picture is that the infinite volume estimates of $\bar{q}_{\max}$, $\sqrt{\overline{q^2}}$ and $\overline{|q|}$ agree. Figure 7 shows the MF and DS fits for these quantities. For L a log scale is used to exhibit $L\to\infty$ clearly, and the infinite volume estimates are depicted towards the end off the scale. With the previously determined zero-temperature exponent the DS values are indeed consistent. For the MF fits $\overline{|q|}_\infty < \sqrt{\overline{q^2}}_\infty < \bar{q}^\infty_{\max}$, as it should be. It is notable that fitting with a wrong zero-temperature exponent may produce entirely inconsistent results. For instance, with $y=0.2$ one finds $\overline{|q|}_\infty > 1 > \bar{q}^\infty_{\max}$.

C. Ground-state energy and entropy

Energy and entropy are self-averaging quantities, in contrast to the observables of the previous subsection. Consequently, the $L=12$ lattices may contribute sufficiently accurate results and we rely now on all four data sets. To check that the self-averaging property is indeed consistent with our data, we have performed fits of the form $L^3\sigma^2(\cdot)=a_1+a_2L^{-3}$ for the energy and entropy variances $\sigma^2(e)$ and $\sigma^2(s)$. The corresponding goodness of fits, reported in Table II are entirely satisfactory.

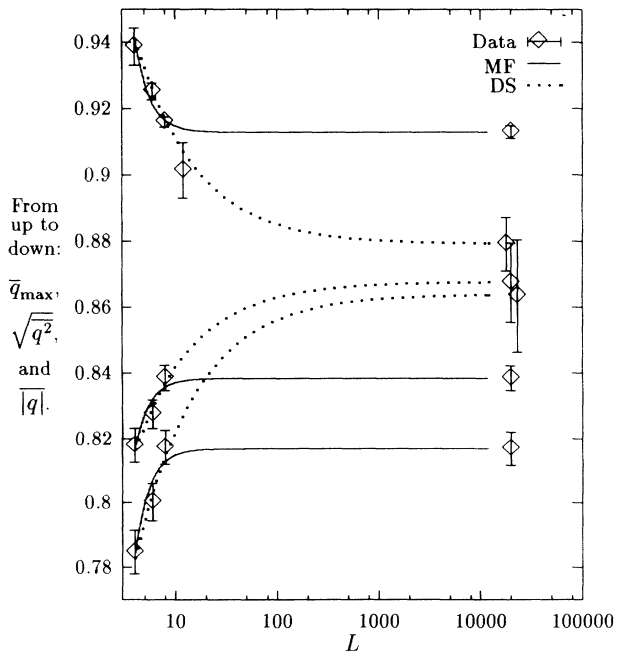

FIG. 7. Fits and extrapolations for $\bar{q}_{\max}$, $\sqrt{\overline{q^2}}$, and $\overline{|q|}$. They rely either on the mean-field (MF) or on the droplet scaling (DS) scenario (the $L=12$ data are not included for these fits).

Most interesting are the FSS fits for the ground-state energy. With $L=12$ included, the MF fit with 1/Volume corrections, $-e_L=a_1+a_2L^{-3}$ is ruled out ($Q=10^{-5}$), whereas the DS fit $-e_L=a_1+a_2L^{-y}$ with $y=0.72$ is well consistent. The DS ground-state energy estimate

$$e=-1.8389\pm0.0040 \tag{13a}$$

is considerably lower than results reported in the literature, $e=-1.75$,[34] $e=-1.76\pm0.02$ (Ref. 35), and $e=-1.7863\pm0.0028$.[29] The latter discrepancy comes because our now very accurate data on lattices with $L\le 8$ rule out the previously used fit with 1/Volume corrections. We like to remark that finding better (lower) ground-state energies for the $L=12$ lattices (we noticed some problems with our present estimates[32]), would only amplify the discrepancy with the MF fit, as the $L=12$ ground-state energies would become even lower compared to the reliable other lattice sizes. This result is our strongest trend in favor of the DS and against the MF scenario. Unfortunately, there is still a catch to it. It may well be that the corrections to the uncritical MF behavior are exponentially small. Although FSS corrections for larger systems would then be greatly reduced, the disadvantage at the present level is that the appropriate $-e_L=a_1+a_2\exp(-a_3L)$ fit has three free parameters. A consistent fit

$$e=-1.7956\pm0.0042\ , \tag{13b}$$

$a_2=-0.21\pm0.04$, $a_3=0.33\pm0.06$, and $Q=0.19$ is then still possible. All three fits are pictured in Fig. 8. The sharp turnover, necessary for the exponential fit looks rather unnatural. Again, accurate data on lattices up to $L=16$ would unambiguously allow to differentiate this behavior from DS. But in contrast to results for the Parisi order parameters, it may be sufficient to simulate a fairly small number of lattices with $L\ge 12$.

Our final remarks address the ground-state entropy. Its multicanonical calculations follows the lines of Ref. 23. Already Kirkpatrick[34] noticed that the exact $J_{ij}=\pm1$ degeneracy of the quenched random variables implies that free single-spin flips are possible for about 5% of the ground-state spins. This implies a large ground-state degeneracy even for realizations for which the Parisi order-parameter distribution has a two-peak structure, as in one of the cases depicted in Fig. 3. Overlaps will be smeared out over a q range $\sim V^{-1/2}$. Consequently either of our scenarios will have a nonzero ground-state entropy, and we expect noncritical 1/Volume corrections. Table II reports that this fit works indeed well, and our infinite volume estimate for the ground-state entropy per spin is

$$s=0.044\,12\pm0.000\,46\ . \tag{14}$$

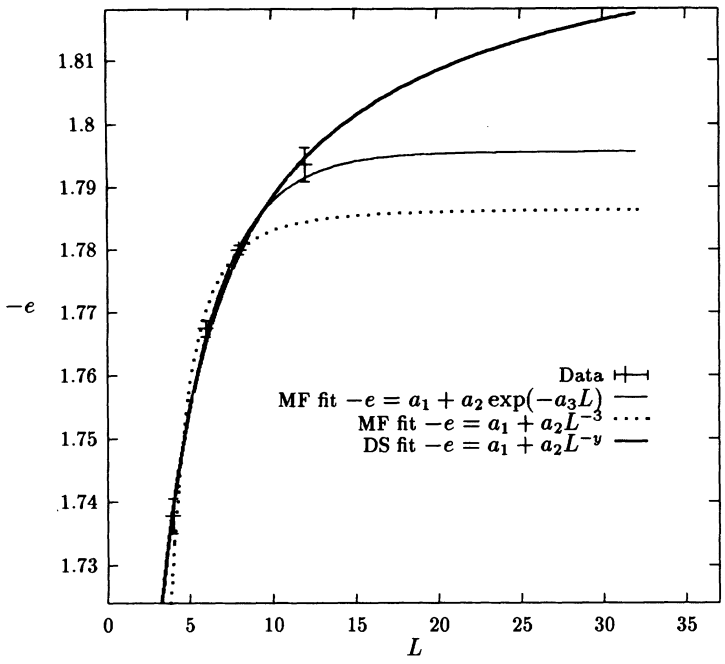

FIG. 8. Fits for the ground-state energy (from up to down: DS, MF with exponentially small corrections, and MF with 1/volume corrections).

This is considerably lower than the "historical" estimate $s = 0.062$,[34] and in agreement with other literature $s = 0.04 \pm 0.02$,[35] $s = 0.046 \pm 0.002$.[29]

IV. SUMMARY

The DS ansatz is so far consistent, and in particular also supported by results for the ground-state energy. For the particular model our investigation presents the first MC estimate of the zero-temperature scaling exponent, which then enters self-consistently into a number of other estimates. Obviously, our lattices are too small to allow a definite infinite volume extrapolation. In particular, the MF picture is still a valid alternative. It is clear that, either by brute computer power or by algorithmic improvements, simulations on larger lattices will become feasible. It seems we are approaching a numerical conclusion about the correct ground-state picture of the 3D EAI model.

ACKNOWLEDGMENTS

We would like to thank David Huse for useful communications, and Claus Vohwinkel for comments on the manuscript. Our simulations were performed on the SCRI cluster of fast workstations. This research project was partially funded by the Department of Energy under Contract Nos. DE-FG05-87ER40319, DE-FC05-85ER2500, and by MK Research, Inc.

[1] M. Mézard, G. Parisi, and M. A. Virasoro, *Spin Glass Theory and Beyond* (World Scientific, Singapore, 1987).
[2] A. P. Young, Phys. Rev. Lett. **51**, 1206 (1983).
[3] A. P. Young, J. D. Reger, and K. Binder, in *The Monte Carlo Method in Condensed Matter Physics*, edited by K. Binder, Topics in Applied Physics Vol. 71 (Springer, New York, 1992).
[4] R. N. Bhatt and A. P. Young, Phys. Rev. Lett. **54**, 924 (1985).
[5] A. T. Ogielski and I. Morgenstern, Phys. Rev. Lett. **54**, 928 (1985).
[6] A. T. Ogielski, Phys. Rev. B **32**, 7384 (1985).
[7] R. N. Bhatt and A. P. Young, Phys. Rev. B **37**, 5606 (1988).
[8] E. Marinari, G. Parisi, and F. Ritort, J. Phys. A **27**, 2687 (1994).
[9] For the long-range SK model, where every spin interacts with all others, the order-parameter function becomes singular in the limit $T \to 0$ (Ref. 1). This is unlikely to happen for a short-range model like the 3D EAI glass. Still, a similar study at low but finite temperatures would be interesting, but was beyond our present scope.
[10] W. L. McMillan, J. Phys. C **17**, 3179 (1984).
[11] A. J. Bray and M. A. Moore, J. Phys. C **18**, L699 (1985).
[12] D. S. Fisher and D. A. Huse, Phys. Rev. Lett. **56**, 1601 (1986).
[13] A. J. Bray and M. A. Moore, in *Heidelberg Colloquium on Glassy Dynamics*, edited by J. L. van Hemmen and I. Morgenstern, Lecture Notes in Physics Vol. 275 (Springer, New York, 1987).
[14] D. S. Fisher and D. A. Huse, Phys. Rev. B **38**, 386 (1988).
[15] A. Bovier and J. Fröhlich, J. Stat. Phys. **44**, 347 (1986).
[16] S. Caracciolo, G. Parisi, S. Patarnello, and N. Sourlas, J. Phys. (France) **51**, 1877 (1990).
[17] D. A. Fisher and D. A. Huse, J. Phys. I (France) **1**, 621 (1991).
[18] N. Kawashima and N. Ito, J. Phys. Soc. Jpn. **62**, 435 (1993).
[19] R. R. P. Singh and D. A. Huse, J. Appl. Phys. **69**, 5225 (1991).
[20] R. E. Hetzel, R. N. Bhatt, and R. R. P. Singh, Europhys. Lett. **22**, 383 (1993).

[21]B. Berg and T. Neuhaus, Phys. Lett. B **267**, 249 (1991).
[22]B. Berg and T. Neuhaus, Phys. Rev. Lett. **68**, 9 (1992).
[23]B. Berg and T. Celik, Phys. Rev. Lett. **69**, 2292 (1992); Int. J. Mod. Phys. C **3**, 1251 (1992).
[24]B. Berg, Int. J. Mod. Phys. C **3**, 1083 (1992).
[25]G. M. Torrie and J. P. Valleau, J. Comput. Phys. **23**, 187 (1977).
[26]A. P. Lyubartsev, A. A. Martsinowski, S. V. Shevkunov, and P. N. Vorontsov-Velyaminow, J. Chem. Phys. **96**, 1176 (1992).
[27]E. Marinari and G. Parisi, Europhys. Lett. **19**, 451 (1992).
[28]W. Kerler and P. Rehberg, Phys. Rev. E **50**, 4220 (1994).
[29]B. Berg, T. Celik, and U. Hansmann, Europhys. Lett. **22**, 63 (1993).
[30]Details of the actually used recursion, which deviates from Ref. 23, will be given elsewhere.
[31]B. Derrida, Phys. Rev. B **24**, 2613 (1981).
[32]B. Berg and C. Vohwinkel (unpublished).
[33]W. H. Press, B. P. Flannery, S. A. Teukolsky, and W. T. Vetterling, *Numerical Recipes* (Cambridge University Press, Cambridge, 1988).
[34]S. Kirkpatrick, Phys. Rev. B **16**, 4630 (1977).
[35]I. Morgenstern and K. Binder, Z. Phys. B **39**, 227 (1980).

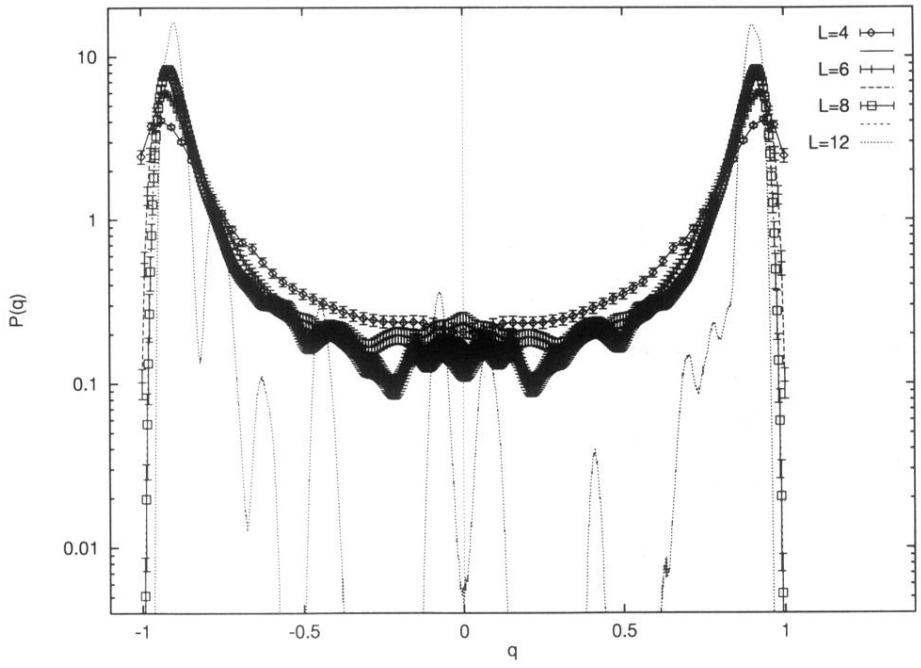

FIG. 2. Probability densities $P(q)$ for the Parisi order parameter ($L=4$, 6, 8, and 12).

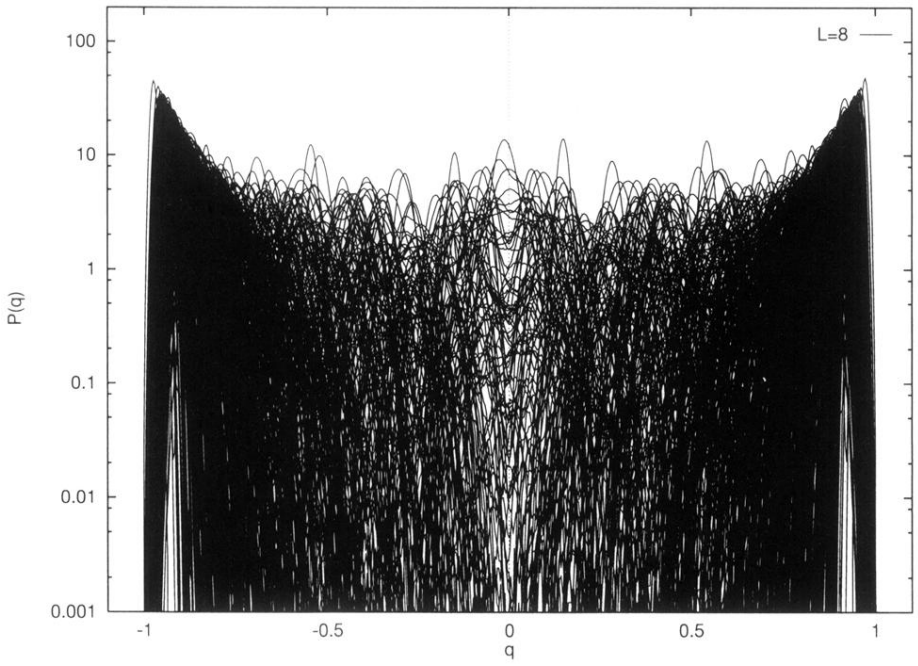

FIG. 4. All $P_j(q)$ probability densities for $L=8$.